

Entanglement-Based Artificial Topology: Neighboring Remote Network Nodes

Si-Yi Chen, Jessica Illiano, Angela Sara Cacciapuoti, *Senior Member, IEEE*,
Marcello Caleffi, *Senior Member, IEEE*

Abstract—Entanglement is unanimously recognized as the key communication resource of the Quantum Internet. Yet, the possibility of implementing novel network functionalities by exploiting the marvels of entanglement has been poorly investigated so far, by mainly restricting the attention to bipartite entanglement. Conversely, in this paper, we aim at exploiting multipartite entanglement as *inter-network resource*. Specifically, we consider the interconnection of different Quantum Local Area Networks (QLANs), and we show that multipartite entanglement allows to dynamically generate an inter-QLAN *artificial topology*, by means of local operations only, that overcomes the limitations of the physical QLAN topologies. To this aim, we first design the multipartite entangled state to be distributed within each QLAN. Then, we show how such a state can be engineered to: i) interconnect nodes belonging to different QLANs, and ii) dynamically adapt to different inter-QLAN traffic patterns. Our contribution aims at providing the network engineering community with a hands-on guideline towards the concept of *artificial topology and artificial neighborhood*.

Index Terms—Entanglement, Quantum Networks, Quantum Communications, Quantum Internet

I. INTRODUCTION

Although the design of the Quantum Internet is at its infancy and early-stage conceptualization [1], there exists a widespread agreement on entanglement being the key resource for the Quantum Internet [2]–[8].

Despite this consensus, entanglement has been poorly investigated so far from the perspective of designing novel networking functionalities [9], [10]. Indeed, existing literature mainly focused on the problem of distributing bipartite entanglement (i.e., EPR pairs) [11] between remote network nodes via quantum repeaters [12], which combine entanglement swapping and entanglement purification to extend entanglement over end-to-end paths, as discussed in [13].

Yet, entanglement does not limit to EPR pairs. In fact, multipartite entanglement – i.e., entanglement shared between more than two parties – represents a powerful resource for quantum communications [9], [13]–[17]. In this paper we exploit such a resource for one of the fundamental tasks of the network layer, namely, the interconnection of remote nodes.

The authors are with the www.QuantumInternet.it research group, *FLY: Future Communications Laboratory*, University of Naples Federico II, Naples, 80125 Italy. A.S. Cacciapuoti and M. Caleffi are also with the Laboratorio Nazionale di Comunicazioni Multimediali, National Inter-University Consortium for Telecommunications (CNIT), Naples, 80126, Italy.

Angela Sara Cacciapuoti acknowledges PNRR MUR NQSTI-PE00000023, Marcello Caleffi acknowledges PNRR MUR project RESTART-PE00000001.

A preliminary shorter version of this work is currently under review for IEEE conference publication.

Specifically, entanglement enables a new form of connectivity, referred to as *entanglement-enabled connectivity* [9], [13], which enables half-duplex unicast links between pairs of nodes sharing entanglement, regardless of their relative positions within the underlying physical network topology. Thus, the entanglement-enabled proximity builds an overlay topology – referred to in the following as *artificial topology* – where pair of nodes are connected via artificial links despite their physical proximity, as long as they share some form of entanglement.

In this context, multipartite entanglement represents an unparalleled communication resource, which allows to decide on-demand – i.e., at run-time – the identities of the nodes interconnected within the artificial topology.

Thus, we consider the interconnection of different Quantum Local Area Networks (QLANs) as building-block of the Quantum Internet, as depicted in Fig. 1, and we engineer multipartite entangled states distributed in each QLAN. The aim is to obtain an inter-QLAN artificial topology, where multiple artificial links among remote nodes are dynamically generated according to the traffic demands, overcoming so the constrained imposed by the physical topology.

Remarkably, we show that multiple artificial links can be dynamically obtained among remote nodes belonging to different QLANs, by means of local operations only, i.e., via free operations from a quantum communication perspective.

Departing from traditional literature on multipartite entanglement – concerning, as instance, the analysis of their quantum properties such as their amount of entanglement [17]–[19] and their *pairability* [20]–[23] – our contribution aims at providing the network engineering community with a hands-on guideline towards the concept of artificial topology and artificial neighborhood.

A. Related work

Within the context of multipartite entangled states for quantum networks, graph states have been recently exploited for an all-photonic implementation of quantum repeaters [24]. Besides, a particular class of multipartite entangled states, namely the 2D cluster states, has been proposed as network resource to be distributed for “routing” EPRs through network nodes. Specifically, the *X-protocol* proposed in [21] for 2D grid networks which aims at extracting an EPR between two remotenodes by leaving part of the remaining graph state intact. Stemming from this results, in [11] the authors discuss how to obtain multiple EPRs from a cluster state among

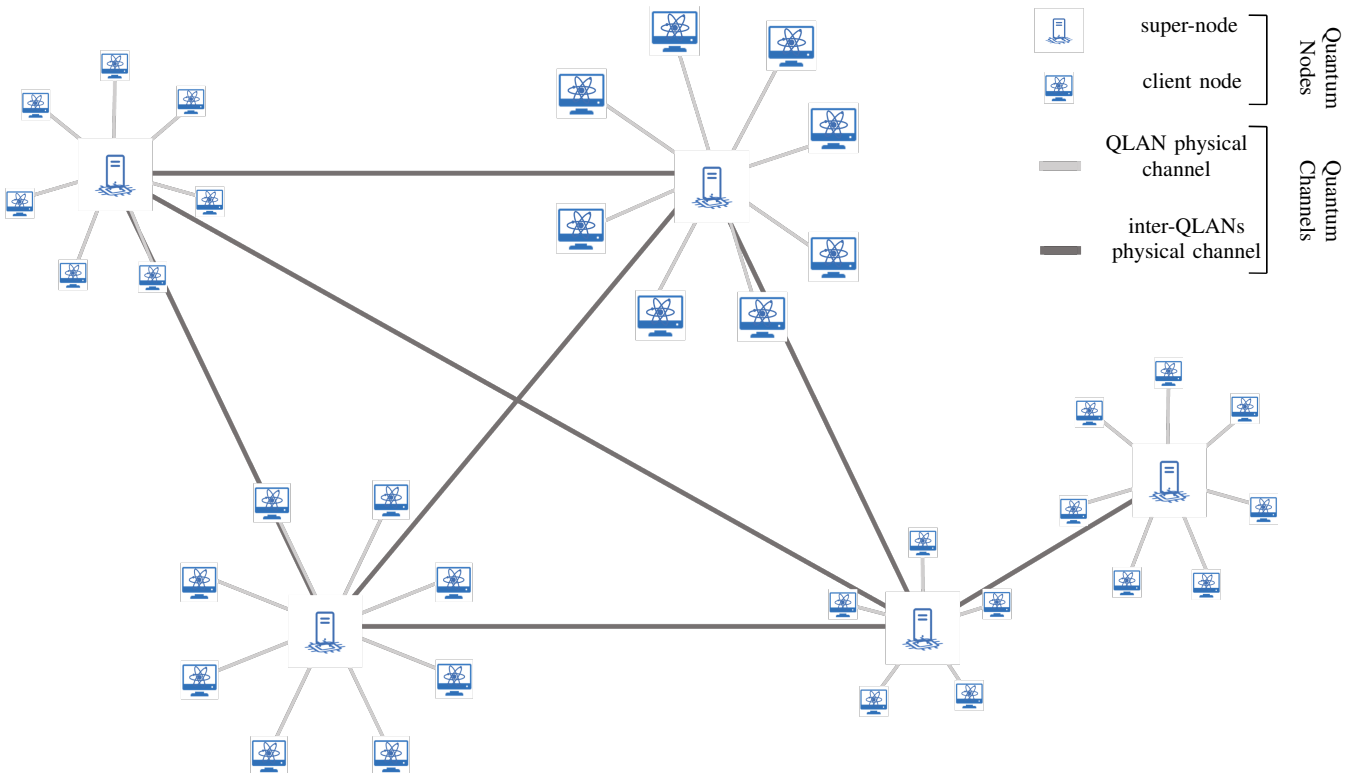


Fig. 1: Schematic representation of the considered quantum network architecture. The network comprises several Quantum Local Area Networks (QLANS). Within each QLAN, a super-node generates and distributes resources – namely, multipartite entangled states – to a set of quantum nodes – referred to as *clients* – with a star-like topology. Inter-QLAN connectivity is enabled by point-to-point quantum channels interconnecting different super-nodes.

diagonal paths by leveraging the X-protocol. Differently, some works focused on the impact of noise on the distribution of multipartite entangled states [25], [26] as well as on the extraction of EPRs from a multipartite state previously shared between network nodes [22]. Additionally, in [27] the LC-orbits of graph states are exploited to minimize the number of EPR required for their distribution.

Remarkably, our main goal is not to extract EPR pairs or explore applications on a given network architecture, differently, we aim at engineering a multipartite entangled state able to easily adapt to different traffic patterns. As a consequence, rather than focusing on the number of EPR pairs consumed or extracted, we focus on the features of the topologies arising from multipartite entanglement. Specifically, we aim at enabling an inter-QLANs artificial topology that can be easily tailored to different traffic patterns by local operations only.

The rest of this paper is organized as follows. In Sec. II we provide the reader with the preliminary concepts about graph theory, graph states and the description of operations on graph states. In Sec. III we present the system model by detailing the considered network architecture as well as the distribution of the considered graph states. In Sec. IV we discuss our main results, by proving a discussion of the choice of the initial multipartite entangled state distributed in each QLAN. Then, we show that multiple artificial links can be dynamically obtained among remote nodes belonging to different QLANs,

by means of local operations only. Finally, in Sec. V we conclude the paper.

II. PRELIMINARIES

A. Graph Theory Basics

A graph is a collection of vertices¹ interconnected by edges, and it is formally defined as the pair $G = (V, E)$ of the two (finite) sets of vertices V and edges $E \subseteq V^2$, respectively.

Remark. In the following, we will restrict our attention on *finite* graphs, namely, graphs with finite V and E . Furthermore, we will consider *undirected* and *simple* graphs, since these two properties are required for the mapping between graphs and graph states [18], [28], as analyzed in the following subsection. We further highlight that *undirected* and *simple* graphs correspond to graphs with un-directed edges², i.e., $(x, y) \equiv (y, x)$, and with edges that cannot connect the same vertex, i.e., $E \subseteq V^2 \triangleq \{(x, y) : x, y \in V \wedge x \neq y\}$.

Whenever two vertices i and j are the endpoints of an edge (i, j) , the two vertices are defined as *adjacent*. We

¹We resort to graph theory for modeling a communication network. Hence, in the following, we equivalently refer to vertices as nodes, by assuming that each vertex models a network node and an edge models an artificial link, i.e., shared entanglement constituting a quantum communication resource between nodes. The mapping between vertices and nodes is defined in Sec. IV-A.

²In the following, with a small notation abuse, we denote un-directed edges as (i, j) – rather than with angle brackets as $\{i, j\}$ – for notation simplicity.

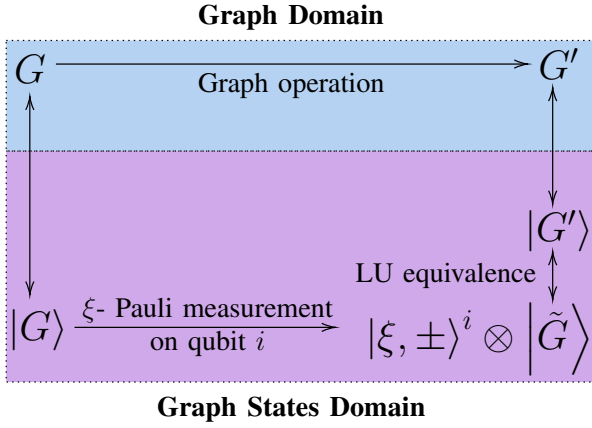


Fig. 2: Schematic diagram of the correspondence between *graph domain* and *graph state domain*, i.e. of the mapping between projective measurements through Pauli operators on graph states and transformations of the associated graphs.

equivalently refer to adjacent vertices as neighbour nodes, as in the following.

Definition 1 (Neighborhood). Given a graph $G = (V, E)$ and a vertex $i \in V$, the neighborhood of i is the set N_i of vertices adjacent to i :

$$N_i = \{j \in V : (i, j) \in E\}. \quad (1)$$

Definition 2 (Induced Subgraph). Given a graph $G = (V, E)$ and a subset of vertices $A \subseteq V$, the *subgraph induced by subset A* , denoted with $G[A]$, is the graph having: i) as vertices, the set A , and ii) as edges, the edges in E that have both endpoints in A . Formally:

$$G[A] = (A, E_A), \quad (2)$$

with $E_A \triangleq \{(i, j) \in E : i \in A \wedge j \in A\}$.

Whether the subset of vertices A is the neighborhood N_i of some vertex i , then $G[N_i]$ is referred to as the *subgraph induced by the neighborhood of i* .

Definition 3 (Complete Graph). A complete graph of order $n = |V|$ is a graph K_n such that every pair of vertices is adjacent:

$$K_n = (V, V^2). \quad (3)$$

In the following, given two vertex sets $A, B \subseteq V$, we widely use the symbol $A \times B \subseteq V^2$ to denote the set of all the possible edges having one endpoint in A and the other in B :

$$A \times B \triangleq \{(i, j) \in V^2 : i \in A \wedge j \in B\} \subseteq V^2. \quad (4)$$

Definition 4 (Graph Complementation). The complement (or inverse) of a graph $G = (V, E)$ is the graph $\tau(G) = (V, \bar{E})$ defined on the same vertex set V , such that two vertices of $\tau(G)$ are adjacent *iff* they are not adjacent in G . Formally:

$$\tau(G) = (V, \bar{E}), \quad (5)$$

with \bar{E} given by:

$$\bar{E} \triangleq V^2 \setminus E = \{(i, j) \in V^2 : (i, j) \notin E\}. \quad (6)$$

Graph complementation can be done also with respect to the subgraph $G[N_i]$ induced by the neighbourhood N_i of vertex i . In this case, it is usually referred to as *local complementation of G at vertex i* and denoted as $\tau_i(G)$.

Definition 5 (Local Complementation). Given a graph $G = (V, E)$, the *local complement of G at vertex i* is the graph $\tau_i(G)$ obtained by complementing the subgraph $G[N_i]$ induced by neighbourhood N_i of vertex i , while leaving the rest of the graph unchanged:

$$\tau_i(G) = (V, (E \cup N_i^2) \setminus E_{N_i}) \quad (7)$$

with E_{N_i} defined in Def. 2.

Definition 6 (Vertex Deletion). The deletion of a vertex i from a graph $G = (V, E)$ generates a new graph, denoted with a small notation abuse as $G - i$, which is obtained by removing both vertex i and all the edges connecting i with its adjacent vertices:

$$G - i = (V \setminus \{i\}, E \setminus (\{i\} \times N_i)) \quad (8)$$

Hence, the edge-set of $G - i$ is the set of edges in G without the edges with vertex i as endpoint.

B. Graph States

Graph states constitute a notable class of multipartite entangled states from a network engineering perspective [18], [29]. As suggested by their name, graph states can be effectively described with the graph theory tools introduced in Sec.II-A. Specifically, stemming from an arbitrary graph G , the corresponding *graph state* – denoted with $|G\rangle$ – can be obtained by mapping each vertex of the graph G with a qubit in the state $|+\rangle$, and by performing a Controlled-Z (CZ) gate between each pair of qubits corresponding to adjacent vertices in G [29].

Remark. The rationale underlying such a mapping lies in the correspondence between graph edges and interaction patterns among the qubits belonging to the composite entangled system. In the mapping, vertices play the role of physical systems and edges represent their interactions.

We recall that the CZ operation is an entangling operation. As a consequence, the distribution of a graph state among remote nodes of a quantum network establishes an entanglement-based connectivity among remote nodes.

Formally, the graph state $|G\rangle$ associated to graph $G = (V, E)$ can be expressed as³:

$$|G\rangle = \prod_{(i,j) \in E} \text{CZ}_{(i,j)} |+\rangle^{\otimes n} \quad (9)$$

with $|+\rangle = \frac{|0\rangle + |1\rangle}{\sqrt{2}}$, $n = |V|$ and $\text{CZ}_{(i,j)}$ denoting the CZ gate applied to the qubits associated to the neighbours $i, j \in V$.

A graph state $|G\rangle$ uniquely corresponds to a graph G . This means that two different graphs G and G' do not describe the same graph state. However, graph states of two different

³With a (widely-used) notation abuse in (9), since the application of the $\text{CZ}_{(i,j)}$ gate on the state $|+\rangle^{\otimes n}$ requires a reference to $n - 2$ identity operations I acting on all the qubits different from i or j .

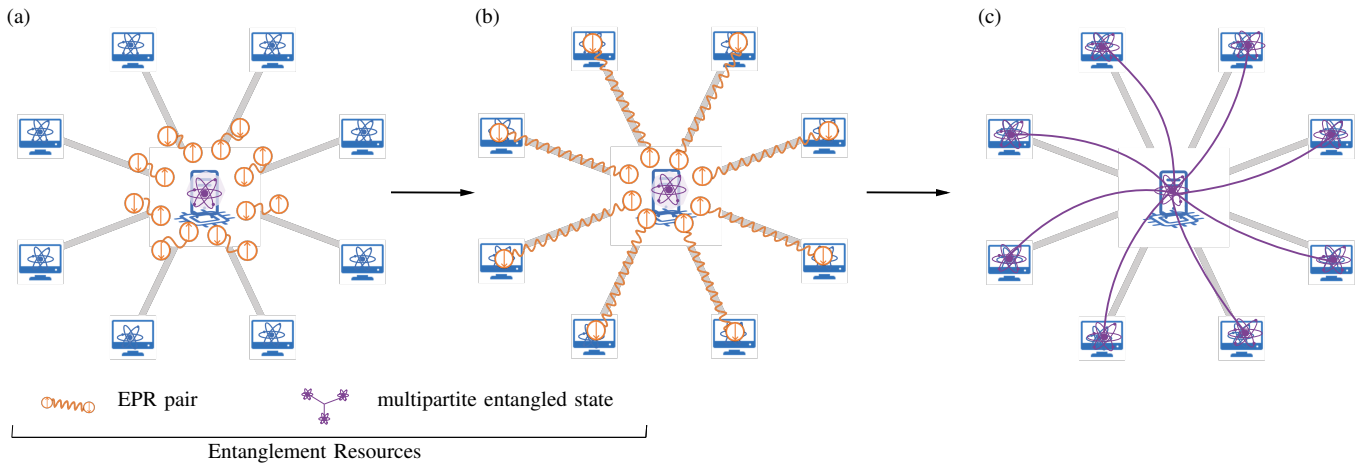


Fig. 3: Pictorial representation of the multipartite entanglement distribution process within a single QLAN of Fig. 1. (a) The super-node is responsible for entanglement generation and distribution within each QLAN. Accordingly, it locally generates the multipartite entanglement state and distribute it via teleportation. For this, one EPR pair per client must be generated at the super-node. (b) Once an EPR pair is shared between super-node and each client, one e-bit of the multipartite entangled state can be teleported to the client by consuming such an EPR. (c) Eventually, the multipartite entangled state is distributed to the clients so that all the QLAN nodes, including the super-node, are entangled.

graphs might be equivalent accordingly to some criteria, determining some equivalence classes among such states. From a network engineering perspective, an equivalency class of interest is represented by the so-called *local unitary* (LU) equivalence, since local unitaries do not change the amount of entanglement. Hence they do not change the communication resources available at the network nodes.

Definition 7 (LU equivalence). Given two n -qubit quantum states, say $|G\rangle$ and $|G'\rangle$, then $|G\rangle$ and $|G'\rangle$ are LU-equivalent iff there exists n local-unitary operators $\{U_i\}$ so that [30]:

$$|G\rangle = \bigotimes_i U_i |G\rangle \quad (10)$$

The mapping between graph states and graphs is of a paramount importance, beyond the expression given in (9) and, hence beyond a merely representation purpose. Specifically, the action of fundamental operations – such as Pauli measurements – on a graph state $|G\rangle$ can be described via simple transformations on the associated graph G .

More into details, a projective measurement through one of the Pauli operators – namely, σ_x , σ_y , or σ_z – on a qubit of the graph state $|G\rangle$ yields to a new graph state $|\tilde{G}\rangle$ on the unmeasured qubits. Interestingly, as proved in [18], [29], this new graph state $|\tilde{G}\rangle$ can be obtained – up to local unitaries – by means of simple transformations on the graph G associated to the original graph state $|G\rangle$, such as vertex deletion and the local complementation introduced in Defs. 6 and 5, respectively. More precisely, the new graph state $|\tilde{G}\rangle$ is LU equivalent to the graph state $|G'\rangle$, obtained by performing the transformations on the graph G associated to the original graph state $|G\rangle$. This is illustrated in Fig. 2.

Since projective measurements through Pauli operators are exploited in Sec. III for engineering the artificial connectivity

enabled by entanglement, it is convenient to summarize their effects on an arbitrary graph state $|G\rangle$ [18], [29].

Pauli Measurements. The projective measurement via a Pauli operator σ_ξ^i on the i -th qubit of the graph state $|G\rangle$ – namely, on the qubit associated to vertex i in graph G – yields to a new graph state $|\tilde{G}\rangle$ among the unmeasured qubits, which is LU-equivalent to the graph state $|G'\rangle$ associated to the graph G' obtained with vertex deletion and local complementations:

$$G' \equiv \begin{cases} G - i & \text{if } \sigma_\xi^i = \sigma_z \\ \tau_i(G) - i & \text{if } \sigma_\xi^i = \sigma_y \\ \tau_{k_0}(\tau_i(\tau_{k_0}(G)) - i) & \text{if } \sigma_\xi^i = \sigma_x. \end{cases} \quad (11)$$

In (11), $k_0 \in N_i$ denotes an arbitrary neighbor of vertex i . For more details please refer to [28].

III. SYSTEM MODEL

A. Network Topology

We consider, as the archetype of the future Quantum Internet, the network resulting from the interconnection of different Quantum Local Area Networks (QLANs) [28].

Entanglement generation is a complex hardware-demanding task, that becomes even more challenging when it comes to multipartite entanglement. For this, as commonly adopted in literature [31]–[35], it is pragmatic to assume each QLAN organized in a star-like physical topology, as represented in Fig. 1, with a set of *clients* connected to a specialized *super-node*, which is responsible for entanglement generation and distribution. Accordingly, multipartite entangled states are generated locally at each super-node, and then distributed to the corresponding clients via teleportation process, as represented

⁴With a mild notation abuse, the dependence on qubit i is omitted for the sake of notation simplicity.

in Fig. 3. The rationale for this strategy – i.e., for distributing multipartite entanglement via teleportation rather than via direct transmission – lies in the higher robustness against losses and tolerance to different persistence levels exhibited by different classes of multipartite states [35]–[37].

While intra-QLAN topologies are pragmatically assumed as star-like physical topologies for the reasons above, no constraints are enforced to inter-QLAN physical connectivity, which is enabled by quantum links interconnecting different super-nodes as shown in Fig. 1.

B. Problem Statement

Stemming from the network architecture introduced so far, we can now formally define our problem, by focusing on the toy-model constituted by two QLANs interconnected by a single physical link between the corresponding super-nodes. We highlight that we develop our analysis in a worst-case scenario, namely the scenario where for each use of this channel, only an EPR pair can be distributed.

Problem. *Given two QLANs, interconnected by a single physical link between the corresponding super-nodes, the goal is to design and engineer a multipartite entanglement state distributed in each QLAN so that artificial links among nodes belonging to different QLANs can be dynamically obtained on-demand, by overcoming so the constraints induced by the physical topologies.*

In essence, an **artificial link** represents a virtual communication link established between two remote nodes, since they share some entanglement. If, as instance, the two nodes shares an EPR pair, then they can exploit such a maximally entangled state for fulfilling a communication task – such as the transmission of a qubit via teleportation – even though they are not connected by a physical quantum link.

In EPR-based networks, artificial links between distant nodes can be obtained by relying only on bipartite entanglement and thus by performing swapping operations at intermediate nodes [5] so that an EPR pair between remote nodes is eventually obtained. Yet, this strategy presents a drawback: the identities of the nodes to be artificially linked must be decided a-priori. In other words, for each EPR pair⁵ distributed through the inter-QLAN link only one artificial link among distant nodes can be obtained. This implies that artificial links via entanglement swapping is reminiscent of *reactive* classical routing strategies, where the source-destination path is discovered when a packet is ready to be transmitted.

Conversely, in multipartite-based networks, multiple artificial links between distant nodes can be obtained by properly choosing the initial multipartite state and by wisely manipulating it via local operations – i.e., via *free operations* from a quantum communication perspective. Hence it is possible to built an *artificial network topology* interconnecting multiple remote nodes via multiple artificial links upon the physical topologies. In such a way, we can pro-actively generate and

⁵Hereafter, we obviously refer to maximally-entangled EPR pairs, neglecting any noise affecting the EPR generation and distributing for the sake of exposition simplicity.

distribute entanglement among subset of nodes of different QLANs so that the identities of the nodes eventually communicating can be chosen dynamically at run time. Clearly, this strategy is reminiscent of *proactive* classical routing strategies, where source-destination paths are discovered in advance, and they remain ready to be used eventually, when the necessity of transmitting a packet arises.

Remark. The artificial topology will be eventually manipulated – without the need of further quantum communications – when a communication request will be ready to be served by extracting the ultimate artificial link interconnecting the effective source-destination pair. Indeed, it may be useful to clarify that an artificial link between two network nodes denotes the “possibility” of extracting a shared EPR between the two nodes, starting from a multipartite entangled state shared among a larger set of nodes. However, the number of EPR pairs that can be simultaneously extracted from a single multipartite entangled state heavily depends on the type and structure of the considered state, and some of the artificial links are depleted during the extraction process.

IV. NEIGHBORING REMOTE NODES

A. Engineering Multipartite Entanglement

As anticipated, we aim at engineering the entanglement-based artificial topology for *neighboring distant nodes*, namely, for creating artificial links among network nodes belonging to different QLANs. To this aim, the choice of the initial multipartite entangled state distributed in each QLAN is of paramount importance.

As discussed in Sec. II-B, we focus our attention on graph states due to the useful mapping between operations on a graph state $|G\rangle$ and transformations of the associated graph G . Yet, graph states represents a wide class of multipartite entangled states. In the next sections, we design and manipulate a specific class of graph states that allows us to enable multiple artificial links among distant nodes belonging to different QLANs. Before formally introducing this specific graph state in Def. 11, the following preliminaries are needed.

More into details, the so-called *chromatic number* of a graph denotes the lowest number of colors needed for coloring⁶ the vertices of a graph, so that no adjacent vertices are colored with the same color. Graphs with chromatic number equal to k are often defined as *k-colorable*, and in the following we formally define two-colorable graphs, also referred to as *bipartite graphs*.

Definition 8 (Two-colorable Graph or Bipartite Graph). A graph $G = (V, E)$ is two-colorable if the set of vertices V can be partitioned⁷ into two subsets $\{P_1, P_2\}$ so that there exist no edge in E between two vertices belonging to the same

⁶In general, coloring assigns labels – namely, colors – to elements of a graph according to arbitrary partition constrains. In the following, we adopt the most widely-used partition constraint based on vertex adjacency, since other coloring problems can be transformed into vertex coloring instances.

⁷A partition of a set is a grouping of its elements into non-empty subsets, so that every element is included in exactly one subset. Formally, the sets $\{P_i\}$ are a partition of V if: i) $P_i \neq \emptyset \forall i$, ii) $\bigcup_i P_i = V$, iii) $P_i \cap P_j = \emptyset \forall i \neq j$.

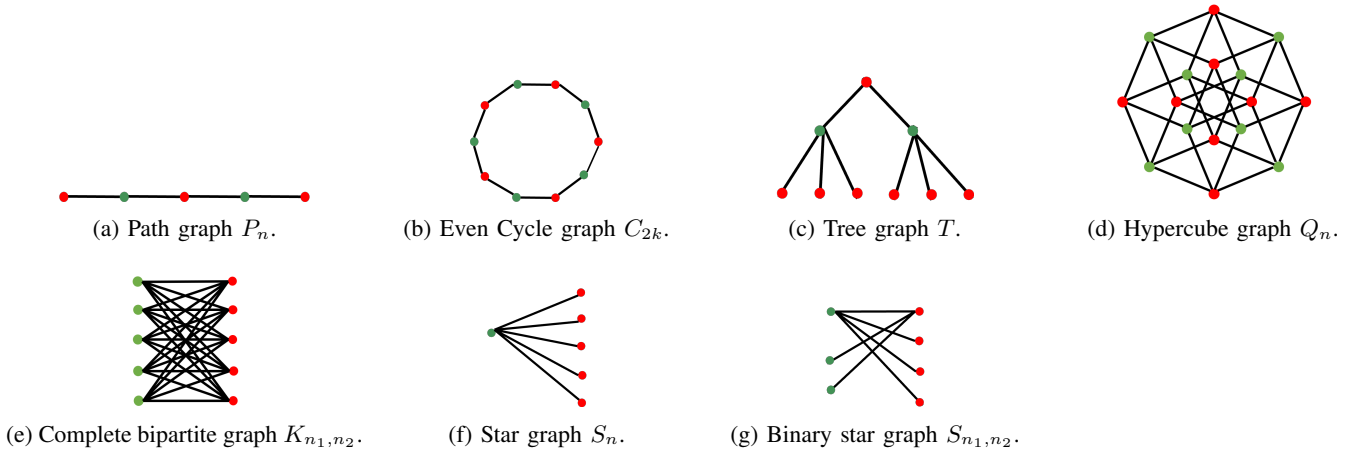


Fig. 4: Notable examples of two-colorable graphs. (a) Path graph P_n . (b) Even cycle graph C_{2k} , consisting of a cycle graph with an even number $n = 2k$ of vertices. (c) Tree graph T , corresponding to an undirected graph in which any two vertices are connected by exactly one path. (d) Hypercube graph Q_n , formed by the 2^n vertices and the $2^{n-1}n$ edges of an n -dimensional hypercube. (e) Complete bipartite graph K_{n_1, n_2} , see Def. 9. (f) Star graph S_n , see Def. 10. (g) Binary star graph S_{n_1, n_2} , see Def. 11.

subset. Two-colorable graph $G = (V, E)$ can also be denoted as $G = (P_1, P_2, E)$.

Remark. We focus our attention on two-colorable graph states without loss of generality, since any graph state can be converted in a two-colorable one under relaxed conditions [18]. Indeed, any graph is two-colorable iff it does not contain cycles of odd length. Furthermore, two-colorable graphs model a wide range of different network topologies. Notable examples of two-colorable graphs are represented in Fig. 4. These include the path-graph, the even cycle graph and the star graph, which represent relevant network topologies – i.e., bus, ring and star [28] – commonly investigated within the classical networking framework. Furthermore, more complex topologies such as tree and hypercube are two-colorable graphs as well.

In the following, we will label the vertices in P_1 and P_2 as follows, for the sake of notation simplicity:

$$P_1 = \{v_1^1, \dots, v_{n_1}^1\} \quad (12)$$

$$P_2 = \{v_1^2, \dots, v_{n_2}^2\} \quad (13)$$

with $n_1 + n_2 = n$.

Definition 9 (Complete Bipartite Graph). Let $G = (P_1, P_2, E)$ be a bipartite graph with $|P_1| = n_1$ and $|P_2| = n_2$. If $E = P_1 \times P_2$, i.e., if

$$\forall v_i^1 \in P_1 \wedge v_j^2 \in P_2, \exists (v_i^1, v_j^2) \in E, \quad (14)$$

G is defined as *complete bipartite graph* and denoted as K_{n_1, n_2} .

Hence, in a complete bipartite graph, any vertex belonging to one part is connected to every vertex belonging to the complementary part by one edge, as shown in Fig. 4e.

Definition 10 (Star Graph). Let K_{n_1, n_2} be a complete bipartite graph. If n_1 (or equivalently n_2) is equal to 1 – namely, if one part is composed by a single vertex – then the

graph is called *star graph* and denoted equivalently as either $K_{1, n-1}$ or S_n , where $n-1$ is the cardinality of the other part. From (14), it results:

$$E = v_1^1 \times P_2 \quad (15)$$

and v_1^1 is referred to as the *center* of the star graph.

QLAN Entanglement Resource. The star graph state $|S_n\rangle$ associated to a star graph S_n shown in Fig. 4f represents the multipartite entangled state generated and distributed in each QLAN, with each qubit of state $|S_n\rangle$ distributed to a different node. Specifically, by following the labelling of (12) and (13), qubit corresponding to vertex v_1^1 is stored at the super-node, whereas qubits corresponding to vertices $\{v_1^2, \dots, v_{n-1}^2\}$ are distributed to the clients.

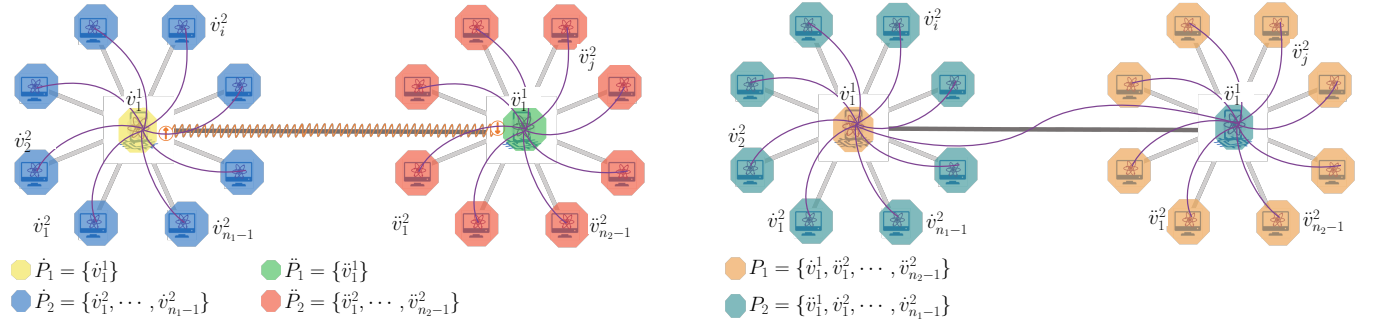
Such a state corresponds to a graph that perfectly matches with the QLAN physical topology and it is easy to generate [32], [34], [38]. It is worthwhile to mention that it represents the worst-case scenario, since from a star graph it is possible to extract only one EPR pair, thus limiting the communication dynamics within the single QLAN. Despite this, in the next sections we will prove that by properly manipulating the multipartite states in the different QLANs, the limitations of the physical topologies can be overcome.

Stemming from the concept of star graph S_n , we are ready now to introduce a two-colorable graph that will be extensively used in the following, and referred to as *binary star graph* S_{n_1, n_2} .

Definition 11 (Binary Star Graph). A binary star graph S_{n_1, n_2} is a bipartite graph $G = (P_1, P_2, E)$ with the edge set E defined as:

$$E = \{v_1^1\} \times P_2 \cup P_1 \times \{v_1^2\} \quad (16)$$

with P_1 and P_2 given in (12) and (13), respectively.



(a) Each super-node generates and distributes, as described in Fig. 3, a star graph state in each QLAN, denoted as $|\dot{S}_{n_1}\rangle = (\dot{P}_1, \dot{P}_2, \dot{E})$ and $|\dot{S}_{n_2}\rangle = (\dot{P}_1, \dot{P}_2, \dot{E})$, respectively. Furthermore, an EPR is shared between the two super-nodes.

(b) By exploiting the EPR shared between the two QLANs for performing a remote CZ, a new graph state shared among all the nodes of the two QLANs is obtained. Remarkably, also this new graph state is a two-colorable graph state, and specifically it is a binary star graph $|S_{n_1, n_2}\rangle$.

Fig. 5: Interconnecting two QLANs through a binary graph state $|S_{n_1, n_2}\rangle$ distributed among all the nodes, obtained from two star graphs distributed in each QLAN and an EPR pair shared between the two super-nodes. A preeminent feature of the distributed state $|S_{n_1, n_2}\rangle$ is that the qubits associated with the vertices of one part – say P_1 – are distributed so that: i) one qubit is at super-node of rightmost QLAN, and ii) the remaining qubits are at clients of the leftmost QLAN.

From (16), it results that only one vertex in each part of a binary star graph – namely, $v_1^1 \in P_1$ and $v_1^2 \in P_2$ – is fully connected, as shown in Fig. 4g.

In Sec IV-B, we will show that – by locally manipulating at some specific network nodes a binary star state $|S_{n_1, n_2}\rangle$ shared between the two QLANs – artificial links among remote nodes are dynamically generated. Yet, before operating on such a state, the state must be distributed among all the nodes. Hence, one preliminary question naturally arises: *how expensive is – from a quantum communication perspective – distributing such a state within the two QLANs?* Or, in other words, how many EPR pairs must be consumed for distributing such a state? One might believe that the required number of EPR pairs should somehow depend on the number of artificial links that must be generated among remote nodes belonging to different QLANs.

We answer to this question with the following proposition.

Proposition 1. *Let's assume that a star state $|\dot{S}_{n_1}\rangle$ has been distributed in the first QLAN and that another star state $|\dot{S}_{n_2}\rangle$ has been distributed in the second QLAN. Then, a binary star state $|S_{n_1, n_2}\rangle$ can be distributed among all the nodes by consuming only one EPR pair at the two super-nodes.*

Proof: Please refer to App. A. ■

Fig. 5 depicts the building process of the binary star state, by also labelling each network node with the vertex-label corresponding to the associated qubit. We can now define our global entanglement resource.

Inter-QLAN Entanglement Resource. *The binary star state $|S_{n_1, n_2}\rangle$ represents the inter-QLAN multipartite entangled resource, which is locally manipulated at network nodes by dynamically enabling multiple artificial links among remote nodes.*

B. Dynamic Artificial Links

Here, we show that multiple artificial links can be dynamically obtained among remote nodes belonging to different QLANs, by means of local operations only, by overcoming the limitations induced by the physical inter-QLAN physical connectivity. Specifically, the set of employed operations limits to single qubit gates, single qubit Pauli measurements and classical communications, which all represent *free operations* from a quantum communication perspective.

To this aim, we consider three different archetypes summarizing different traffic patterns, namely:

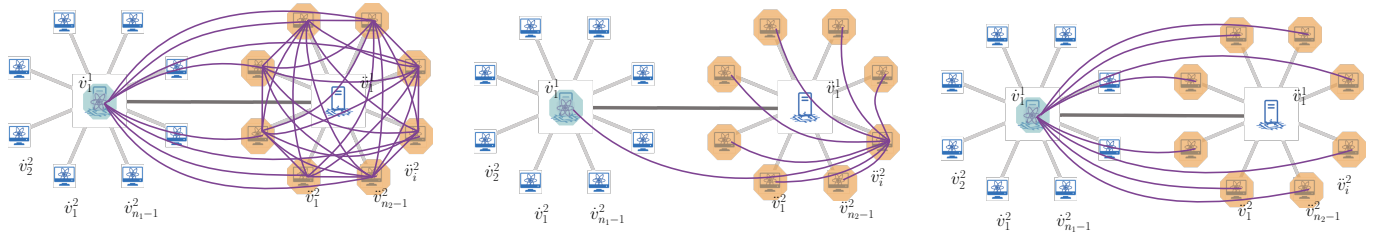
- i) *peer-to-peer*,
- ii) *role delegation*
- iii) *clients hand-over*

and for each archetype we discuss different artificial topologies that equivalently satisfy the communication demand.

Proposition 2 (Hierarchical Peer-to-Peer). *Starting from a binary star graph state $|S_{n_1, n_2}\rangle$ shared between $n = n_1 + n_2$ nodes belonging to two different QLANs, a n_i -complete graph state $|K_{n_i}\rangle$ (with $i = 1, 2$) shared between the super-node of a QLAN and all the $(n_i - 1)$ -clients of the other QLAN can be obtained.*

Proof. Please refer to App. B. □

The effect of Prop. 2, depicted in Fig. 6a, is particularly relevant from a communication perspective. Specifically, the obtained complete (i.e., fully connected) graph is LU-equivalent to a GHZ state, which allows the deterministic extraction of one EPR pair between *any couple* of nodes sharing it. As a consequence, the complete graph obtained exhibits a remarkable flexibility on the choice of the identities of the nodes exploiting the ultimate artificial link, aka the extracted EPR. Notably, the completely connected graph includes the other QLAN super-node. Hence, from a topological perspective, the involved clients and super-node act as peer-to-peer



(a) *Hierarchical peer-to-peer* artificial topology discussed in Prop. 2: an artificial fully-connected topology among all the clients of the same QLAN and one super-node of a different QLAN.

(b) *Role delegation type I* artificial topology discussed in Cor. 1: an artificial star topology among the same set of nodes of Fig. 6a, but centered at a client of the same QLAN.

(c) *Clients hand-over* artificial topology discussed in Cor. 2: an artificial star topology among the same set of nodes of Fig. 6a, but centered at a super-node of a different QLAN.

Fig. 6: Different artificial inter-QLAN topologies matching with a traffic pattern involving the super-node of one QLAN and clients of the other QLAN. Remarkably, all the artificial inter-QLAN topologies are obtained by manipulating a binary star graph state with local operations and measurements only.

entities, which can exploit the shared entangled state either to accommodate intra-QLAN traffic requests or inter-QLAN traffic requests. This consideration induced us to label this proposition as “hierarchical peer-to-peer” artificial topology, by including the differentiation – aka hierarchy – in terms of hardware requirements between clients and super-node.

It is worthwhile to mention that the “Hierarchical Peer-to-Peer” artificial topology is particularly advantageous whenever no information is available on the actual network traffic features of the QLAN clients. Specifically, if a client may equally need to communicate with clients belonging to the same QLANs or with clients belonging to a different QLAN, then the communication request will be ready to be served by proactively manipulating the “hierarchical peer-to-peer” artificial topology. And, remarkably, the communication request is easily served by simply performing local unitaries and measurements, without any additional quantum communication.

Furthermore, from Prop. 1 two further results follow.

Corollary 1 (Role Delegation Type I). *Starting from a binary star graph state $|S_{n_1, n_2}\rangle$ shared between $n = n_1 + n_2$ nodes belonging to two different QLANs, a n_i -star graph state $|S_{n_i}\rangle$ (with $i = 1, 2$) centered at one QLAN client node and connecting all the remaining $(n_i - 2)$ -clients of the same QLAN and the super-node of the other QLAN can be obtained.*

Proof. Please refer to App. D. \square

The result of Cor. 1 is represented in Fig. 6b with the client node \check{v}_i^2 being the center of the star graph. By looking at both Fig. 6a and Fig. 6b it is evident that – differently from the “hierarchical peer-to-peer” artificial topology exhibiting $\frac{n_i(n_i-1)}{2}$ artificial links – the “role delegation” artificial topology provides less degrees of freedom in selecting the identities of the nodes that can proactively extract the ultimate artificial link. However, this is not less advantageous as the star graph comes in handy whenever the traffic pattern likely involves a specific client node \check{v}_i^2 , which may equally need to communicate with clients belonging to its QLANs or need a link outside its QLAN. Due to the particular structure of this artificial topology – having one client as center of the star

graph instead of the super-node – we were induced to label this topology as “role delegation” topology of type I. Indeed, a different type of role delegation topology, named type II, is introduced in Cors. 3 and 4.

Another remarkable corollary of Prop. 2 is the possibility of building the so-called “clients hand-over” artificial topology between two QLANs, as detailed in the following corollary.

Corollary 2 (Clients Hand-Over). *Starting from a binary star graph state $|S_{n_1, n_2}\rangle$ shared between $n = n_1 + n_2$ nodes belonging to two different QLANs, a n_i -star graph state $|S_{n_i}\rangle$, (with $i = 1, 2$) centered at one QLAN super-node and connecting all the $(n_i - 1)$ -clients of the other QLAN can be obtained.*

Proof. Please refer to App. E. \square

We note that, accordingly to Cor. 2, artificial links are built between a super-node of one QLAN and the clients of a different QLAN, as shown in Fig 6c. This, from a topological perspective, is equivalent to virtually *move* the clients of a QLAN into a different QLAN, resembling thus a sort of *clients hand-over* from one QLAN to the other.

Remark. As proved in the Appendices, the artificial topologies represented in Fig. 6 are obtained by leveraging suitable sequences of Pauli measurements, which, thus, represent a tool for engineering the artificial connectivity. To elaborate more, the graph represented in Fig. 6a leverages a sequence of Pauli- z and Pauli- y measurements. Remarkably, by replacing the Pauli- y measurement at the super-node with a Pauli- x measurement, we obtain the LU-equivalent graph state corresponding to a star graph among all the nodes, as shown in Fig. 6b. A Pauli- x measurement is equivalent to the sequence of graph operations given in (11) that involves the arbitrary neighbor k_0 . And indeed k_0 represents an engineering parameter. In fact, by choosing a client as k_0 – as instance, say $k_0 = \check{v}_i^2$ – we obtain a graph state corresponding to a star graph centered at \check{v}_i^2 as shown in Fig. 6b. Differently, if we set $k_0 = \check{v}_1^1$, the star graph is centered at \check{v}_1^1 , as shown in Fig. 6c.

From the above, it may be concluded that only artificial topologies involving super-node and clients can be built upon the binary star graph state $|S_{n_1, n_2}\rangle$. The following Prop. 3 and the subsequent Cors. 3 and 4 prove, instead, that artificial topologies involving only clients belonging to different QLANs can be built by properly manipulating the binary star graph state.

Proposition 3 (Pure Peer-to-Peer). *Starting from a binary star graph state $|S_{n_1, n_2}\rangle$ shared between $n = n_1 + n_2$ nodes belonging to two different QLANs, a n_i -complete connected graph state $|K_{n_i}\rangle$, with $i = 1, 2$, shared between one client node of a QLAN and all the $(n_i - 1)$ -clients of the other QLAN can be obtained.*

Proof. Please refer to App. F. \square

As shown in Fig. 7a, Prop. 3 allows an arbitrary client belonging to a QLAN to share an artificial link with any client belonging to a different QLAN. Hence, it generates an artificial QLAN topology among *peer* client entities – thus, the naming “pure” – by neighbouring remote nodes, despite the original constraints imposed by the physical topologies.

Indeed, a pure peer-to-peer artificial topology extends the flexibility on the choice of the identities of the nodes exploiting the ultimate artificial link, by involving only clients at different QLANs. This could be particularly advantageous for designing distributed network functionalities relying on clients communication capabilities. Indeed, if a client needs to communicate with a client belonging to a different QLAN, then – by proactively manipulating the artificial topology – the communication request is ready to be served, without further orchestration at the super-node. Indeed, the communication request is fulfilled by performing local unitaries without any additional quantum communications. And, actually, the client of the other QLAN can be selected by properly manipulating the initial binary star graph. Hence their identities can be engineered on-demand.

Corollary 3 (Role Delegation Type II - Case 1). *Starting from a binary star graph state $|S_{n_1, n_2}\rangle$ shared between $n = n_1 + n_2$ nodes belonging to two different QLANs, a n_i -star graph state $|S_{n_i}\rangle$ (with $i = 1, 2$) centered at one QLAN client node and connecting all the remaining $(n_i - 2)$ -clients of the same QLAN and a client node of the other QLAN can be obtained.*

Proof. Please refer to App. G. \square

Similarly to Corollary 1, due to the particular structure of this artificial topology shown in Fig. 7b – which has one client as center of the star graph instead of the super-node – we are induced to label this topology as “role delegation topology type II”, since (differently from type I) no super-node is connected within the star graph. A different realization of this topology – labeled as “case 2” for distinguish from the previous one that is labeled as “case 1” – is derived with the following corollary.

Corollary 4 (Role Delegation Type II - Case 2). *Starting from a binary star graph state $|S_{n_1, n_2}\rangle$ shared between $n =$*

$n_1 + n_2$ nodes belonging to two different QLANs, a n_i -star graph state $|S_{n_i}\rangle$ (with $i = 1, 2$) centered at one QLAN client node and connecting all the $(n_i - 1)$ clients of the other QLAN can be obtained.

Proof. Please refer to App. H. \square

The result of this corollary establishes that artificial links are built between a client of one QLAN and all the clients of the other QLAN, as shown in Fig. 7c. This topology comes in handy whenever a client node v_j^2 needs to communicate with clients belonging to a different QLAN.

Remark. The theoretical results established via Props. 2 and 3 and their corollaries make evident that it is possible to overcome the constraints imposed by the physically topologies by locally and properly manipulating engineered multipartite entangled states, without any further use of quantum links. This is equivalent to neighbour remote nodes, where the concept of neighboring is not meant in terms of physical proximity via physical links, but it rather should be intended – as discussed in [9] – as “*entangled proximity*”.

The degrees of freedom offered by the binary star graph to select the identities of the nodes sharing the ultimate artificial link are further highlighted by the following proposition and its subsequent corollary.

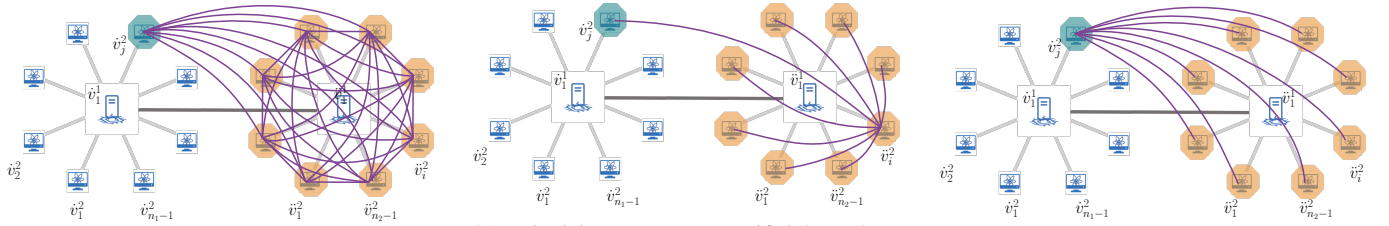
Proposition 4 (Extranet). *Starting from a binary star graph state $|S_{n_1, n_2}\rangle$ shared between $n = n_1 + n_2$ nodes belonging to two different QLANs, a $(n_1 + n_2 - 2)$ -complete bipartite graph state $|K_{n_1-1, n_2-1}\rangle$, shared between all the $(n_1 - 1)$ -clients of one QLAN and all the $(n_2 - 1)$ -clients of the other QLAN can be obtained.*

Proof. Please refer to App. I. \square

Remark. The effects of the result in Prop. 4, depicted in Fig. 8a, are particularly relevant from a communication perspective. Specifically artificial links are created among clients belonging to different QLANs. Thus, inter-QLANs communication needs can be promptly fulfilled, by selecting on-demand – i.e. accordingly to the traffic patterns – the identities of the clients sharing the ultimate artificial link. With respect to the topology in Fig. 7c, it is evident that the degrees of freedom in selecting these identities are higher. This comes without paying the price of additional quantum communications, but only by engineering the proper local operations to be performed – in such a case – at the super-nodes. This, from a topological perspective, can be saw as obtaining an “extranet” interconnecting all the clients of the two original “intranets”, thus the name.

Corollary 5 (Double Role Delegation). *Starting from a binary star graph state $|S_{n_1, n_2}\rangle$ shared between $n = n_1 + n_2$ nodes belonging to two different QLANs, a $(n_1 + n_2 - 2)$ -binary star graph state $|S_{n_1-1, n_2-1}\rangle$ shared between the $(n_1 - 1)$ -clients of one QLAN and the $(n_2 - 1)$ -clients of the other QLAN, centered at one client from each QLAN, can be obtained.*

Proof. Please refer to App. J. \square

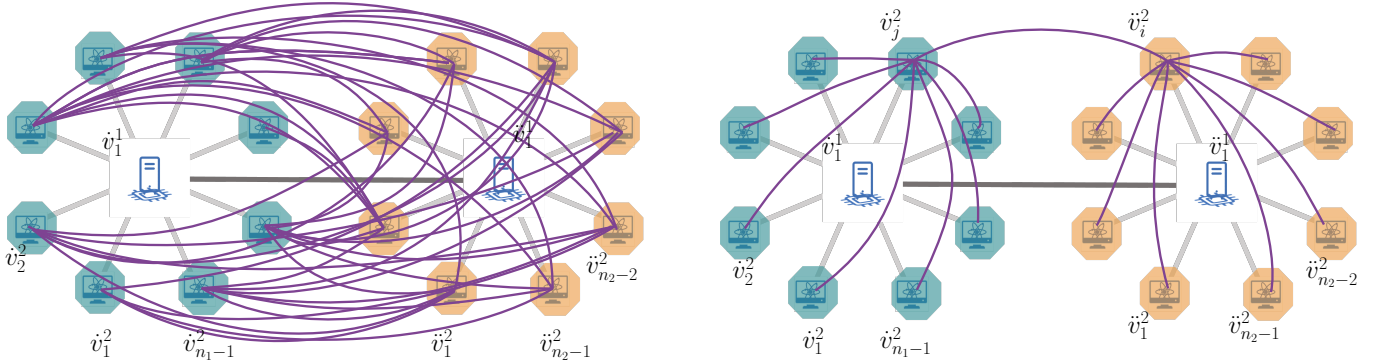


(a) *Pure peer-to-peer* artificial topology discussed in Prop 3 : an artificial fully-connected topology among all the clients of the same QLAN and one client node of a different QLAN.

(b) *Role delegation type II* artificial topology, case 1, discussed in Cor. 3: an artificial star topology among the same set of nodes of Fig. 7a, but centered at a client of the rightmost QLAN.

(c) *Role delegation type II* artificial topology, case 2, discussed in Cor. 4: an artificial star topology among the same set of nodes of Fig. 7a, but centered at a client of a different QLAN.

Fig. 7: Different artificial inter-QLAN topologies matching with a traffic pattern involving one client of one QLAN and clients of the other QLAN. Remarkably, the action of “sacrificing” the artificial link between the two QLAN super-nodes enables inter-QLAN peer-to-peer artificial topologies particular useful for designing distributed network functionalities relying on client communication capabilities.



(a) *Extranet* artificial topology discussed in Prop. 4: an artificial complete bipartite topology interconnecting each client of one QLANs with each client of the other QLAN.

(b) *Double Role Delegation* artificial topology discussed in Cor. 5: an artificial binary star topology among the same set of clients of Fig. 8a, centered at two client nodes belonging to two different QLANs.

Fig. 8: Different artificial inter-QLAN topologies matching with a traffic pattern potentially involving all the clients of the two QLAN. The two topologies represent two LU-equivalent graph states that can be obtained by leveraging different local operations. Although LU-equivalent, the two artificial topologies are able to accommodate different client traffic patterns.

The result of Cor. 5, depicted in Fig. 8b, extends the dynamics offered by the artificial topology in Fig. 7b. Indeed, differently from the “extranet” topology, with the “*double role delegation*” artificial topology both intra-QLAN and inter-QLAN traffic demands can be accommodate. The price is having less degree of freedom in selecting the identities of the clients sharing the ultimate artificial link.

V. CONCLUSIONS

The goal of this paper is to provide an operational and easy-to-use guide for understanding and manipulating the artificial topology enabled by multipartite entangled states, with the aim to facilitate the design and engineering of quantum communication protocols. As a consequence, we departed from the traditional combinatorial study of graph states, to focus on the theoretical analysis of different artificial inter-QLAN

topologies. Such topologies are enabled by the proper manipulation of two-colorable graph states via local operations, and they are able to accommodate different inter-QLAN traffic patterns. We underline that our contribution should be intended as hands-on guideline for the network engineering community to recognize the marvels – with no-classical counterpart – enabled by entanglement for networking and inter-networking tasks.

APPENDIX A PROOF OF PROPOSITION 1

Let us label the vertices of the graphs $\dot{S}_{n_1} = (\dot{P}_1, \dot{P}_2, \dot{E})$ and $\ddot{S}_{n_2} = (\ddot{P}_1, \ddot{P}_2, \ddot{E})$, associated to the graph states $|\dot{S}_{n_1}\rangle$ and $|\ddot{S}_{n_2}\rangle$ distributed in the first and second QLANs respec-

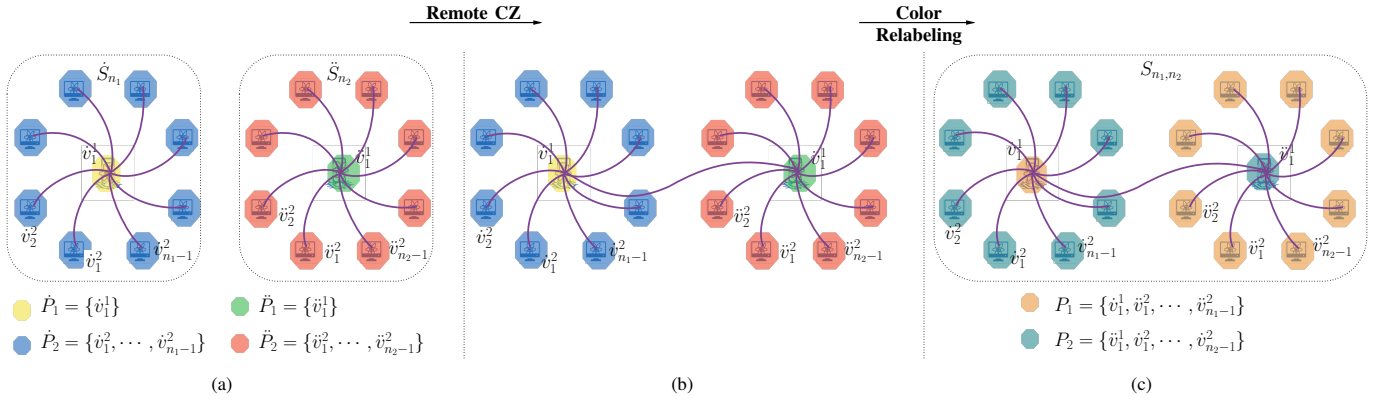


Fig. 9: Generation of a *binary star state* starting from two *star states* distributed in each QLAN, with physical topology (quantum links) omitted for the sake of simplicity. (a) Initial scenario where three entangled resources are shared: i) star state $|\dot{S}_{n_1}\rangle$ among QLAN1 nodes, ii) star state $|\dot{S}_{n_2}\rangle$ among QLAN2 nodes, and iii) an EPR pair between the two super-nodes \dot{v}_1^1 and \dot{v}_1^2 . (b) By consuming the EPR shared between the two super-nodes, a remote CZ operation is performed. This results in the generation of the additional edge $(\dot{v}_1^1, \dot{v}_1^2)$, represented by the purple wavy line. (c) By re-coloring the overall graph, it becomes evident that it is a two-colorable graph corresponding to the binary star graph state $|S_{n_1, n_2}\rangle$.

tively, according to (12) and (13):

$$\dot{P}_1 = \{\dot{v}_1^1\} \wedge \dot{P}_2 = \{\dot{v}_1^2, \dots, \dot{v}_{n_1-1}^2\}, \quad (17)$$

$$\ddot{P}_1 = \{\ddot{v}_1^1\} \wedge \ddot{P}_2 = \{\ddot{v}_1^2, \dots, \ddot{v}_{n_2-1}^2\}, \quad (18)$$

with $\dot{E} = \dot{P}_1 \times \dot{P}_2$ and $\ddot{E} = \ddot{P}_1 \times \ddot{P}_2$. Accordingly and as shown in Fig. 9-a, the qubits of graph state $|\dot{S}_{n_1}\rangle$ are distributed among the nodes of the first QLAN, with the super-node storing the qubit associated to vertex \dot{v}_1^1 and the clients storing the qubits associated to $\dot{v}_1^2, \dots, \dot{v}_{n_1-1}^2$. Similarly, the qubits of the graph state $|\dot{S}_{n_2}\rangle$ are distributed among the nodes of the second QLAN, with the super-node storing the qubit associated to the vertex \dot{v}_1^2 and the clients storing the qubits associated to $\dot{v}_1^1, \dots, \dot{v}_{n_2-1}^1$. By consuming an EPR pair, the two super-nodes can perform a CZ operation between the two qubits at their sides, which corresponds to adding edge $(\dot{v}_1^1, \dot{v}_1^2)$ between the associated vertices in the corresponding graph, as shown in Fig. 9-b. Hence, this additional edge connects the (only) vertex in \dot{P}_1 with the (only) vertex in \dot{P}_2 , and it results:

$$E = \dot{E} \cup \ddot{E} \cup \{(\dot{v}_1^1, \dot{v}_1^2)\}. \quad (19)$$

If we want to color the overall graph, then these two vertex sets must be colored with two different colors, say orange and cyan. However, no edges connect the vertex in \dot{P}_1 with vertices in \ddot{P}_2 , and hence all these vertices can be colored with the same color, orange. Similarly, no edges connect vertex in \ddot{P}_1 with the vertices in \dot{P}_2 , hence all these vertices can be colored with the same color. It follows that the overall graph G is a two-colorable graph with parts P_1 and P_2 given by:

$$P_1 = \dot{P}_1 \cup \ddot{P}_2 = \{\dot{v}_1^1, \dot{v}_1^2, \dots, \dot{v}_{n_2-1}^2\} \quad (20)$$

$$P_2 = \ddot{P}_1 \cup \dot{P}_2 = \{\ddot{v}_1^1, \ddot{v}_1^2, \dots, \ddot{v}_{n_1-1}^2\} \quad (21)$$

and with edge-set E in (19). The proof follows by acknowledging that (19) coincides with (16).

APPENDIX B PROOF OF PROPOSITION 2

Let us adopt Fig. 5 labeling and let us suppose that the state $|K_{n_i}\rangle$ to be obtained must interconnect the clients of the right-most QLAN, which implies $n_i = n_2$ ⁸. Accordingly, the final state must be the complete graph state $|K_{n_2}\rangle$, which corresponds to complete graph $K_{n_2} = (P_1, P_1^2)$, with P_1 defined in (20).

The proof follows by performing: i) $(n_1 - 1)$ -Pauli-z measurements on the qubits stored at the clients of QLAN-1, and ii) a Pauli-y measurement on the qubit stored at the super-node of the second QLAN. From (11), it results that the action of $(n_1 - 1)$ -Pauli-z measurements is equivalent to remove all the client vertices in P_2 in (21), which yields to the graph:

$$S_{n_1, n_2} - P_2 \setminus \{\dot{v}_1^1\} = (P_1 \cup \{\dot{v}_1^1\}, P_1 \times \{\dot{v}_1^1\}) = S'_{n_2+1} \quad (22)$$

We observe that the graph S'_{n_2+1} in (22) corresponds to a star graph connecting the vertices in the set $P_1 \cup \{\dot{v}_1^1\}$, with the super-node \dot{v}_1^1 being the center of the star. Then, a Pauli-y measurement is performed on the qubit stored at super-node of second QLAN and associated to the vertex \dot{v}_1^1 . From (11), the action of this measurement is equivalent to the local complementation of the graph S'_{n_2+1} at vertex \dot{v}_1^1 , followed by the deletion of \dot{v}_1^1 from the graph, i.e., $\tau_{\dot{v}_1^1}(S'_{n_2+1}) - \dot{v}_1^1$. Step-by-step, we first perform the local complementation $\tau_{\dot{v}_1^1}(S'_{n_2+1})$, which yields to the graph:

$$\begin{aligned} \tau_{\dot{v}_1^1}(S'_{n_2+1}) &= (P_1 \cup \{\dot{v}_1^1\}, P_1 \times \{\dot{v}_1^1\} \cup N_{\dot{v}_1^1}^2 \setminus E_{N_{\dot{v}_1^1}}) \\ &= (P_1 \cup \{\dot{v}_1^1\}, (P_1 \cup \{\dot{v}_1^1\})^2) \end{aligned} \quad (23)$$

This equals to adding to the edge-set of the star graph S'_{n_2+1} all the possible edges having both endpoints in the subset P_1 . As a result, we obtain the complete graph connecting the set

⁸Clearly, the same final state shared among a set of $n'_i < n_i$ nodes can be obtained straightforwardly, by simply removing the undesired nodes with Pauli-z measurements at their qubits.

$P_1 \cup \{\dot{v}_1^1\}$. We then proceed by removing the super-node \dot{v}_1^1 , and the proof follows:

$$\tau_{\dot{v}_1^1}(S'_{n_2+1}) - \dot{v}_1^1 = (P_1, P_1^2) = K_{n_2}. \quad (24)$$

APPENDIX C

INTERMEDIATE RESULT:

PAULI- x MEASUREMENT AT STAR GRAPH CENTER

In the following, we prove an intermediate result widely used through the remaining appendices, namely, the Pauli- x measurement on the qubit stored at the center of a star graph state. Hence, it is convenient to collect it in a separate appendix for the sake of clarity.

Lemma 1. *Performing an x -measurement of the qubit held at the center \dot{v}_1^1 of a star graph $\dot{S}_{n_1} = (\dot{P}_1, \dot{P}_2, \dot{E})$ with k_0 set equal to \dot{v}_j^2 yields to a new star graph \dot{S}_{n_1-1} among the set of nodes \dot{P}_2 with center node \dot{v}_j^2 .*

Proof: Let us adopt Fig. 5 labeling and let us consider the initial graph \dot{S}_{n_1} as defined in App. A. According to (11), the x -measurement on the qubit corresponding to vertex \dot{v}_1^1 is equivalent to perform the following sequence of graph operations, where we set $k_0 = \dot{v}_j^2$ as from the thesis:

$$\tau_{\dot{v}_j^2}(\tau_{\dot{v}_1^1}(\tau_{\dot{v}_j^2}(\dot{S}_{n_1})) - \dot{v}_1^1). \quad (25)$$

We proceed step-by-step. First, the local complementation at node \dot{v}_j^2 does not alter the graph, i.e., $\tau_{\dot{v}_j^2}(\dot{S}_{n_1}) = \dot{S}_{n_1}$, since the neighborhood $N_{\dot{v}_j^2}$ of \dot{v}_j^2 has cardinality equal to 1. Then, the local complementation at \dot{v}_1^1 adds to the edge-set of \dot{S}_{n_1} all the possible edges among the vertexes in \dot{P}_2 . As a result, the complete graph \dot{K}_{n_1} connecting the set $\dot{P}_2 \cup \{\dot{v}_1^1\}$ is obtained:

$$\begin{aligned} \tau_{\dot{v}_1^1}(\dot{S}_{n_1}) &= (\dot{P}_2 \cup \{\dot{v}_1^1\}, (\dot{P}_2 \times \{\dot{v}_1^1\}) \cup N_{\dot{v}_1^1}^2 \setminus E_{N_{\dot{v}_1^1}}) \\ &= (\dot{P}_2 \cup \{\dot{v}_1^1\}, (\dot{P}_2 \times \{\dot{v}_1^1\}) \cup \dot{P}_2^2) = \dot{K}_{n_1}. \end{aligned} \quad (26)$$

Then, by removing \dot{v}_1^1 , the resulting graph is:

$$\dot{K}_{n_1} - \dot{v}_1^1 = (\dot{P}_2, \dot{P}_2^2) = \dot{K}_{n_1-1}, \quad (27)$$

which corresponds to the complete graph involving the set of nodes \dot{P}_2 . Finally, the local complementation at node \dot{v}_j^2 yields to the graph:

$$\begin{aligned} \tau_{\dot{v}_j^2}(\dot{K}_{n_1-1}) &= (\dot{P}_2, (\dot{P}_2^2 \cup N_{\dot{v}_j^2}^2) \setminus E_{N_{\dot{v}_j^2}}) \\ &= (\dot{P}_2, \{\dot{v}_j^2\} \times (\dot{P}_2 \setminus \{\dot{v}_j^2\})) = \dot{S}_{n_1-1} \end{aligned} \quad (28)$$

where $N_{\dot{v}_j^2}^2 = E_{N_{\dot{v}_j^2}} = \dot{P}_2 \setminus \{\dot{v}_j^2\}$. Accordingly, the local complementation at \dot{v}_j^2 removes from the edge-set of \dot{K}_{n_1-1} all the possible edges among the vertexes in $\dot{P}_2 \setminus \{\dot{v}_j^2\}$ and returns the star graph \dot{S}_{n_1-1} involving the considered nodes with node \dot{v}_j^2 being the center of the star. ■

APPENDIX D

PROOF OF COROLLARY 1

The proof follows by adopting similar reasoning as in Prop. 2. Specifically, we adopt Fig. 5 labeling and we suppose, without any loss in generality, that the star graph state $|\dot{S}_{n_i}\rangle$ has to be shared among all the right-most QLAN clients.

Accordingly, the final star graph state is $|\dot{S}_{n_2}\rangle$, corresponding to the star graph $\dot{S}_{n_2} = (\{\dot{v}_i^2\}, \{\dot{v}_1^1\} \cup \dot{P}_2 \setminus \{\dot{v}_i^2\}, \dot{E})$ with \dot{P}_2 , defined in (18) and with $\dot{E} = \dot{v}_i^2 \times \{\{\dot{v}_1^1\} \cup \dot{P}_2 \setminus \{\dot{v}_i^2\}\}$. Specifically, \dot{S}_{n_2} corresponds to a star graph centered at one arbitrary client \dot{v}_i^2 of second QLAN and connecting the super-node of first QLAN and the remaining clients of second QLAN. The thesis follows by performing: i) $(n_1 - 1)$ -Pauli- z measurements on the qubits stored at the clients of QLAN-1, and ii) a Pauli- x measurement on the qubit stored at the super-node of the second QLAN, by setting k_0 equal to \dot{v}_i^2 . The effects of $(n_1 - 1)$ -Pauli- z measurements are the same as analyzed in App. B, by yielding so to the star graph S'_{n_2+1} in (22). Then, as proved in App. C, the Pauli- x measurement on the qubit \dot{v}_1^1 returns a star graph \dot{S}_{n_2} shared between the set P_1 in (20) and super-node \dot{v}_1^1 with one client node \dot{v}_i^2 in P_1 being the center of the star.

APPENDIX E

PROOF OF COROLLARY 2

The proof follows by adopting similar reasoning as in the proof of Cor. 1, and by setting as arbitrary neighbouring node k_0 the super-node \dot{v}_1^1 .

APPENDIX F

PROOF OF PROPOSITION 3

Similarly to the previous proofs, we adopt Fig. 5 labeling and we suppose, without any loss in generality, that the n_i -complete connected graph state $|K_{n_i}\rangle$ has to be shared between one client node of the first QLAN and all the $(n_2 - 1)$ -clients of the right-most QLAN. Accordingly, $|K_{n_2}\rangle$ corresponds to the complete graph $K_{n_2} = (\{\dot{v}_j^2\} \cup \dot{P}_2, (\{\dot{v}_j^2\} \cup \dot{P}_2)^2)$ with \dot{P}_2 defined in (18). The proof follows by performing: i) $(n_1 - 2)$ -Pauli- z measurements on the qubits stored at the clients of the left-most QLAN, with the exception of the client \dot{v}_j^2 , ii) a Pauli- y measurement at the super-node of the first QLAN, and iii) a Pauli- y measurement at the super-node of the second QLAN. From (11), by performing $(n_1 - 2)$ Pauli- z measurements on the clients of first QLAN is equivalent to remove all the clients in P_2 in (21), except for the client node \dot{v}_j^2 . Thus the resulting graph is:

$$\begin{aligned} S_{n_1, n_2} - (P_2 \setminus \{\dot{v}_j^2\}) &= \\ &= \underbrace{(P_1 \cup \{\dot{v}_j^2, \dot{v}_1^1\})}_{V'} \times \underbrace{P_1 \cup \{(\dot{v}_j^2, \dot{v}_1^1)\}}_{E'} \triangleq G' \end{aligned} \quad (29)$$

Then, a Pauli- y measurement is performed on the qubit – associated to the vertex \dot{v}_1^1 – stored at super-node of the first QLAN. From (11), and by reasoning as in Appendix B, this yields to the graph :

$$\begin{aligned} \tau_{\dot{v}_1^1}(G') - \dot{v}_1^1 &= (V', E' \cup N_{\dot{v}_1^1}^2 \setminus E_{N_{\dot{v}_1^1}}) - \dot{v}_1^1 = \\ &= (V', E' \cup \{\dot{v}_1^1, \dot{v}_j^2\}^2 \setminus \emptyset) - \dot{v}_1^1 = \\ &= (\dot{P}_2 \cup \{\dot{v}_1^1, \dot{v}_j^2\}, \{\dot{v}_1^1\} \times (\dot{P}_2 \cup \{\dot{v}_j^2\})) = S''_{n_2+1} \end{aligned} \quad (30)$$

We observe that the graph S''_{n_2+1} in (30) corresponds to a star graph connecting the set $\dot{P}_2 \cup \{\dot{v}_1^1, \dot{v}_j^2\}$ with super-node \dot{v}_1^1 being the center of the star. Then, a Pauli- y measurement

is performed on the qubit \ddot{v}_1^1 stored at super-node of second QLAN. From (11), this is equivalent to perform the following sequence of graph operations $\tau_{\ddot{v}_1^1}(S''_{n_2+1}) - \ddot{v}_1^1$. Step-by-step, the local complementation yields to the graph:

$$\tau_{\ddot{v}_1^1}(S''_{n_2+1}) = (\ddot{P}_2 \cup \{\dot{v}_j^2, \dot{v}_1^1\}, (\ddot{P}_2 \cup \{\dot{v}_j^2, \dot{v}_1^1\})^2) \quad (31)$$

This equals to adding to the edge-set of the star graph S''_{n_2+1} all the possible edges among the subset \ddot{P}_2 with node $\{\dot{v}_j^2\}$. As a result, we obtain the complete graph connecting the set $\ddot{P}_2 \cup \{\dot{v}_1^1, \dot{v}_j^2\}$, namely, the client nodes of the second QLAN, one client node $\{\dot{v}_j^2\}$ and the super-node of the first QLAN. Then, by removing the super-node \ddot{v}_1^1 , the proof follows:

$$\tau_{\ddot{v}_1^1}(S''_{n_2+1}) - \ddot{v}_1^1 = (\{\dot{v}_j^2\} \cup \ddot{P}_2, (\{\dot{v}_j^2\} \cup \ddot{P}_2)^2) = K_{n_2} \quad (32)$$

APPENDIX G PROOF OF COROLLARY 3

Similarly to the previous proofs, we adopt Fig. 5 labeling and suppose that the state to be obtained is shared among all the right-most QLAN clients. Accordingly, the final state has to be $|S_{n_2}\rangle$ corresponding to star graph $S_{n_2} = (\{\ddot{v}_i^2\}, \{\dot{v}_j^2\} \cup \ddot{P}_2 \setminus \{\dot{v}_i^2\}, E)$, with \ddot{P}_2 , defined in (18) and with $E = \ddot{v}_i^2 \times \{\{\dot{v}_1^1\} \cup \ddot{P}_2 \setminus \{\dot{v}_i^2\}\}$. Thus the star graph is shared between the client node \dot{v}_j^2 of the left-most QLAN and the clients of the right-most QLAN with one client node \ddot{v}_i^2 of right-most QLAN being the center of the star. The proof follows by performing: i) (n_1-2) -Pauli- z measurements on the qubits stored at the clients of the left-most QLAN except at the client \dot{v}_j^2 , ii) a Pauli- y measurement of the super-node of the first QLAN, and iii) a Pauli- x measurement of the super-node of the second QLAN with the arbitrary node k_0 set equal to \ddot{v}_i^2 . By reasoning as in the Appendix F, it is easy to recognize that the graph before the x -measurement at the super-node \ddot{v}_1^1 , is the star graph S''_{n_2+1} expressed in (30). By accounting for this, for the result in Appendix C, and by performing a Pauli- z measurement on \ddot{v}_1^1 , the star graph S_{n_2} with the client node $\ddot{v}_i^2 \in \ddot{P}_2$ being the center of star is obtained by setting $k_0 = \ddot{v}_i^2$.

APPENDIX H PROOF OF COROLLARY 4

The proof follows similarly to Cor. 3, by setting $k_0 = \dot{v}_j^2$.

APPENDIX I PROOF OF PROPOSITION 4

We adopt Fig. 5 labeling again, and the proof follows by performing: i) a Pauli- x measurement on the qubit associated to the vertex \dot{v}_1^1 of the super-node of the first QLAN, with k_0 set equal to \dot{v}_1^1 , and ii) a Pauli- z measurement on the qubit associated to the vertex \ddot{v}_1^1 of the super-node of the second QLAN. From (11), a Pauli- x measurement on \dot{v}_1^1 with $k_0 = \dot{v}_1^1$ is equivalent to perform the sequence of graph operations $\tau_{\dot{v}_1^1}(\tau_{\ddot{v}_1^1}(S_{n_1, n_2})) - \dot{v}_1^1$. Step-by-step, the local complementation at super-node \dot{v}_1^1 adds all the possible edges

having both endpoints belonging to the set P_1 , by yielding to the graph:

$$\tau_{\dot{v}_1^1}(S_{n_1, n_2}) = (P_1 \cup P_2, (P_1 \times \{\dot{v}_1^1\}) \cup (P_2 \times \{\dot{v}_1^1\}) \cup P_1^2). \quad (33)$$

We observe that the neighborhood $N_{\dot{v}_1^1}$ of \dot{v}_1^1 in $\tau_{\dot{v}_1^1}(S_{n_1, n_2})$ is $P_1 \cup P_2 \setminus \{\dot{v}_1^1\}$. Hence, the local complementation at the super-node \dot{v}_1^1 yields to the graph:

$$\tau_{\dot{v}_1^1}(\tau_{\dot{v}_1^1}(S_{n_1, n_2})) = (P_1 \cup P_2, (\{\dot{v}_1^1\} \times P_2) \cup P_2^2 \cup (\ddot{P}_2 \times \dot{P}_2)), \quad (34)$$

where \ddot{P}_2, \dot{P}_2 are defined in (20) and (21). Then, we proceed by removing the super-node \dot{v}_1^1 , which yields to the graph:

$$\tau_{\dot{v}_1^1}(\tau_{\dot{v}_1^1}(S_{n_1, n_2})) - \dot{v}_1^1 = (\ddot{P}_2 \cup P_2, P_2^2 \cup (\ddot{P}_2 \times \dot{P}_2)). \quad (35)$$

We observe that the neighborhood $N_{\ddot{v}_1^1}$ of \ddot{v}_1^1 in (35) corresponds to the set \dot{P}_2 . Hence, the local complementation at the super-node \ddot{v}_1^1 yields to the graph:

$$\begin{aligned} \tau_{\ddot{v}_1^1}(\tau_{\dot{v}_1^1}(\tau_{\dot{v}_1^1}(S_{n_1, n_2})) - \dot{v}_1^1) &= \\ &= (\ddot{P}_2 \cup P_2, (\{\dot{v}_1^1\} \times \dot{P}_2) \cup (\ddot{P}_2 \times \dot{P}_2)) \end{aligned} \quad (36)$$

and the proof follows by performing a Pauli- z measurement on \ddot{v}_1^1 :

$$\begin{aligned} \tau_{\ddot{v}_1^1}(\tau_{\dot{v}_1^1}(\tau_{\dot{v}_1^1}(\tau_{\dot{v}_1^1}(S_{n_1, n_2})) - \dot{v}_1^1) - \ddot{v}_1^1) &= \\ &= (\ddot{P}_2 \cup \dot{P}_2, \ddot{P}_2 \times \dot{P}_2) = K_{n_1-1, n_2-1}. \end{aligned} \quad (37)$$

APPENDIX J PROOF OF COROLLARY 5

Similarly to the previous proofs, we adopt Fig. 5 labeling. The proof follows by performing: i) a Pauli- x measurement on the qubit associated to vertex \dot{v}_1^1 of the super-node of the first QLAN with the arbitrary node k_0 set equal to \dot{v}_j^2 , and ii) a Pauli- x measurement on the qubit associated to vertex \ddot{v}_1^1 of the super-node of the second QLAN with the arbitrary node k_0 set equal to \ddot{v}_i^2 . From (11), a Pauli- x measurement on \dot{v}_1^1 with $k_0 = \dot{v}_j^2$ is equivalent to perform the sequence of graph operations $\tau_{\dot{v}_j^2}(\tau_{\dot{v}_1^1}(\tau_{\ddot{v}_1^1}(S_{n_1, n_2})) - \dot{v}_1^1)$. By reasoning as in the previous appendix, it can be easily verified that one obtains the following graph:

$$\begin{aligned} \tau_{\dot{v}_j^2}(\tau_{\dot{v}_1^1}(\tau_{\ddot{v}_1^1}(S_{n_1, n_2})) - \dot{v}_1^1) &= \\ &= (\underbrace{\ddot{P}_2 \cup P_2}_{\tilde{V}}, \underbrace{(\{\dot{v}_1^1\} \times \dot{P}_2) \cup (\{\dot{v}_j^2\} \times (P_2 \setminus \{\dot{v}_j^2\}))}_{\tilde{E}}) = \tilde{G}. \end{aligned} \quad (38)$$

We then perform a x -measurement on the super-node \ddot{v}_1^1 of second QLAN with the arbitrary node k_0 set equal to \ddot{v}_i^2 . From (11), this is equivalent to perform the following sequence of graph operations:

$$\tau_{\ddot{v}_i^2}(\tau_{\dot{v}_1^1}(\tau_{\ddot{v}_1^1}(\tilde{G})) - \ddot{v}_1^1). \quad (39)$$

Step-by-step, the local complementation at client \tilde{v}_i^2 does not change the graph \tilde{G} . Then the local complementation at super-node \tilde{v}_1^1 yields to the graph:

$$\tau_{\tilde{v}_1^1}(\tilde{G}) = (\tilde{V}, \underbrace{(\{\tilde{v}_j^2\} \times \tilde{P}_2) \cup \tilde{P}_2 \cup \tilde{E}}_{\tilde{E}'}) \quad (40)$$

By removing \tilde{v}_1^1 , the resulting graph is given by:

$$\begin{aligned} \tau_{\tilde{v}_1^1}(\tilde{G}) - \tilde{v}_1^1 &= (\tilde{V} \setminus \{\tilde{v}_1^1\}, \tilde{E}' \cup (\{\tilde{v}_j^2\} \times (\tilde{P}_2 \setminus \{\tilde{v}_j^2\}))) \\ &= \tilde{G}' \end{aligned} \quad (41)$$

The proof follows by observing that the neighborhood $N_{\tilde{v}_i^2}$ of \tilde{v}_i^2 in \tilde{G}' corresponds to the set \tilde{P}_2 . Thus, the local complementation at \tilde{v}_i^2 yields to the graph:

$$\begin{aligned} \tau_{\tilde{v}_i^2}(\tilde{G}') &= (\tilde{P}_2, \tilde{P}_2, (\{\tilde{v}_i^2\} \times \tilde{P}_2) \cup (\{\tilde{v}_j^2\} \times \tilde{P}_2)) = \\ &= S_{n_1-1, n_2-1}. \end{aligned} \quad (42)$$

REFERENCES

- [1] W. Kozłowski, S. Wehner, R. V. Meter, B. Rijsman, A. S. Cacciapuoti, M. Caleffi, and S. Nagayama, "Architectural Principles for a Quantum Internet," RFC 9340, Mar. 2023.
- [2] H. J. Kimble, "The quantum internet," *Nature*, vol. 453, no. 7198, pp. 1023–1030, 2008.
- [3] H. J. Briegel, D. E. Browne, W. Dür, R. Raussendorf, and M. Van den Nest, "Measurement-based quantum computation," *Nature Physics*, vol. 5, no. 1, pp. 19–26, 2009.
- [4] A. S. Cacciapuoti, M. Caleffi, F. Tafuri, F. S. Cataliotti, S. Gherardini, and G. Bianchi, "Quantum internet: Networking challenges in distributed quantum computing," *IEEE Network*, vol. 34, no. 1, pp. 137–143, 2020.
- [5] A. S. Cacciapuoti, M. Caleffi, R. Van Meter, and L. Hanzo, "When entanglement meets classical communications: Quantum teleportation for the quantum internet," *IEEE Transactions on Communications*, vol. 68, no. 6, pp. 3808–3833, 2020, invited paper.
- [6] W. Dür, R. Lamprecht, and S. Heusler, "Towards a quantum internet," *European Journal of Physics*, vol. 38, no. 4, p. 043001, 2017.
- [7] J. Wallnöfer, A. Pirker, M. Zwerger, and W. Dür, "Multipartite state generation in quantum networks with optimal scaling," *Scientific reports*, vol. 9, no. 1, pp. 1–18, 2019.
- [8] J. Miguel-Ramiro and W. Dür, "Delocalized information in quantum networks," *New Journal of Physics*, vol. 22, no. 4, p. 043011, 2020.
- [9] A. S. Cacciapuoti, J. Illiano, and M. Caleffi, "Quantum internet addressing," *IEEE Network*, 2023.
- [10] S.-Y. Chen, A. S. Cacciapuoti, X.-B. Chen, and M. Caleffi, "Multipartite entanglement for the quantum internet," in *IEEE International Conference on Communications*, 5 2023.
- [11] J. Freund, A. Pirker, and W. Dür, "A flexible quantum data bus," *arXiv preprint arXiv:2404.06578*, 2024.
- [12] H.-J. Briegel, W. Dür, J. I. Cirac, and P. Zoller, "Quantum repeaters: The role of imperfect local operations in quantum communication," *Phys. Rev. Lett.*, vol. 81, pp. 5932–5935, Dec 1998.
- [13] J. Illiano, M. Caleffi, A. Manzalini, and A. S. Cacciapuoti, "Quantum internet protocol stack: a comprehensive survey," *Computer Networks*, vol. 213, 2022.
- [14] A. Pirker, J. Wallnöfer, and W. Dür, "Modular architectures for quantum networks," *New Journal of Physics*, vol. 20, no. 5, p. 053054, 2018.
- [15] A. Pirker and W. Dür, "A quantum network stack and protocols for reliable entanglement-based networks," *NJP*, vol. 21, no. 3, p. 033003, mar 2019.
- [16] J. Miguel-Ramiro, A. Pirker, and W. Dür, "Genuine quantum networks with superposed tasks and addressing," *npj Quantum Inf.*, vol. 7, p. 135, 09 2021.
- [17] C. Kruszynska, S. Anders, W. Dür, and H. J. Briegel, "Quantum communication cost of preparing multipartite entanglement," *Physical Review A*, vol. 73, no. 6, p. 062328, 2006.
- [18] M. Hein, W. Dür, J. Eisert, R. Raussendorf, M. Nest, and H.-J. Briegel, "Entanglement in graph states and its applications," *arXiv preprint quant-ph/0602096*, 2006.
- [19] N. Claudet and S. Perdrix, "Covering a graph with minimal local sets," *arXiv:2402.10678*, 2024.
- [20] S. Bravyi, Y. Sharma, M. Szegedy, and R. de Wolf, "Generating k epr-pairs from an n -party resource state," *arXiv:2211.06497*, 2022.
- [21] F. Hahn, A. Pappa, and J. Eisert, "Quantum network routing and local complementation," *npj Quantum Information*, vol. 5, no. 1, p. 76, 2019.
- [22] M. F. Mor-Ruiz and W. Dür, "Influence of noise in entanglement-based quantum networks," *IEEE Journal on Selected Areas in Communications*, 2024.
- [23] M. Cautrès, N. Claudet, M. Mhalla *et al.*, "Vertex-minor universal graphs for generating entangled quantum subsystems," *arXiv:2402.06260*, 2024.
- [24] N. Benchasattabuse, M. Hajdušek, and R. Van Meter, "Architecture and protocols for all-photon quantum repeaters," *arXiv preprint arXiv:2306.03748*, 2023.
- [25] W. Dür and H.-J. Briegel, "Stability of macroscopic entanglement under decoherence," *Phys. Rev. Lett.*, vol. 92, p. 180403, May 2004. [Online]. Available: <https://link.aps.org/doi/10.1103/PhysRevLett.92.180403>
- [26] W. Dür and H. J. Briegel, "Entanglement purification and quantum error correction," *Reports on Progress in Physics*, vol. 70, no. 8, p. 1381, 2007.
- [27] T. Ji, J. Liu, and Z. Zhang, "Distributing arbitrary quantum cluster states by graph transformation," *arXiv preprint arXiv:2404.05537*, 2024.
- [28] F. Mazza, M. Caleffi, and A. S. Cacciapuoti, "Quantum lan: On-demand network topology via two-colorable graph states," *under review*, 2024.
- [29] M. Hein, J. Eisert, and H. J. Briegel, "Multipartite entanglement in graph states," *Physical Review A*, vol. 69, no. 6, p. 062311, 2004.
- [30] B. Kraus, "Local unitary equivalence of multipartite pure states," *Physical review letters*, vol. 104, no. 2, p. 020504, 2010.
- [31] M. Epping *et al.*, "Multi-partite entanglement can speed up quantum key distribution in networks," *New J. Phys.*, 2017.
- [32] G. Avis, F. Rozpędek, and S. Wehner, "Analysis of multipartite entanglement distribution using a central quantum-network node," *Phys. Rev. A*, vol. 107, p. 012609, Jan 2023.
- [33] G. Vardoyan, S. Guha, P. Nain, and D. Towsley, "On the exact analysis of an idealized quantum switch," *ACM SIGMETRICS Performance Evaluation Review*, vol. 48, no. 3, pp. 79–80, 2021.
- [34] L. Bugalho *et al.*, "Distributing multipartite entanglement over noisy quantum networks," *quantum*, vol. 7, p. 920, 2023.
- [35] J. Illiano, M. Caleffi, M. Viscardi, and A. S. Cacciapuoti, "Quantum mac: Genuine entanglement access control via many-body dicke states," *IEEE Transactions on Communications*, 2023.
- [36] E. Rieffel and W. Polak, *Quantum Computing: A Gentle Introduction*. The MIT Press, 2011.
- [37] N. Brunner and T. Vértesi, "Persistency of entanglement and nonlocality in multipartite quantum systems," *Phys. Rev. A*, vol. 86, no. 4, p. 042113, 2012.
- [38] J. Wallnöfer, A. Pirker, M. Zwerger, and W. Dür, "Multipartite state generation in quantum networks with optimal scaling," *Scientific reports*, vol. 9, no. 1, p. 314, 2019.



Si-yi Chen received the Ph.D degree as an outstanding graduate in 2023 in School of Cyberspace Security from Beijing University of Posts and Telecommunications (China). Currently, she is a Postdoctoral fellow in University of Naples Federico II (Italy). She serves as TPC member in IEEE International Conference on Quantum Computing and Engineering 2024. Since 2022, she is a member of the Quantum Internet Research Group, FLY: Future Communications Laboratory in University of Naples Federico II where she works on multiparty quantum networks, long-distance quantum communications and quantum entanglements.



Jessica Illiano (GS'21) Jessica Illiano received the B.Sc degree in 2018 and then the M.Sc degree in 2020 both (summa cum laude) in Telecommunications Engineering from University of Naples Federico II (Italy). In 2020 she was winner of the scholarship "Quantum Communication Protocols for Quantum Security and Quantum Internet" fully funded by TIM S.p.A. and in 2024 she received her PhD degree in Information Technologies and Electrical Engineering at University of Naples Federico II. Since 2017, she is a member of the Quantum Internet

Research Group, FLY: Future Communications Laboratory at the University of Naples Federico II where she currently is a post-doc. Currently, she is website co-chair of N2Women and student Associate Editor for IET Quantum Communication. Her research interests include quantum communications, quantum networks and quantum information processing.



Angela Sara Cacciapuoti (M'10–SM'16) is a faculty at the University of Naples Federico II, Italy. Her work has appeared in first tier IEEE journals and she has received different awards, including the "2022 IEEE ComSoc Best Tutorial Paper Award", the "2022 WICE Outstanding Achievement Award" for outstanding contribution in the quantum communication and network field, and "2021 N2Women: Stars in Networking and Communications". For the Quantum Internet topics, she is a IEEE ComSoc Distinguished Lecturer, class of 2022-2023. Currently,

Angela Sara serves as Editor at Large for IEEE Trans. on Communications and as Editor\ Associate Editor for the journals: IEEE Trans. on Quantum Engineering, IEEE Network and IEEE Communications Surveys & Tutorials. She served as Area Editor for IEEE Communications Letters from 2019 to sept 2023, and she was a recipient of the 2017 Exemplary Editor Award of the IEEE Communications Letters. From 2020 to 2021, Angela Sara was the Vice-Chair of the IEEE ComSoc Women in Communications Engineering (WICE). Previously, she has been appointed as Publicity Chair of WICE. From 2016 to 2019 she has been an appointed member of the IEEE ComSoc Young Professionals Standing Committee. From 2017 to 2020, she has been the Treasurer of the IEEE Women in Engineering (WIE) Affinity Group of the IEEE Italy Section. Her current research interests are mainly in Quantum Communications, Quantum Networks and Quantum Information Processing.



Marcello Caleffi (M'12, SM'16) is an Associate Professor with the DIETI Department, University of Naples Federico II, where he co-lead the Quantum Internet Research Group. He is also with the National Laboratory of Multimedia Communications, National Inter- University Consortium for Telecommunications. From 2010 to 2011, he was with the Broadband Wireless Networking Laboratory with the Georgia Institute of Technology, as a Visiting Researcher. In 2011, he was also with the NaNoNetworking Center in Catalunya (N3Cat) with

the Universitat Politècnica de Catalunya, as a Visiting Researcher. Since July 2018, he held the Italian National Habilitation as a Full Professor of Telecommunications Engineering. His work appeared in several premier IEEE Transactions and Journals, and he received multiple awards, including the best strategy, the most downloaded article, and the most cited article awards. In 2022, he has been awarded with the IEEE Communications Society "Best Tutorial Paper Award" 2022 for the paper "When Entanglement Meets Classical Communications: Quantum Teleportation for the Quantum Internet." He currently serves as an Editor for IEEE Transactions On Wireless Communications and IEEE Transactions On Quantum Engineering. Previously, he served as an Editor/Associate Technical Editor for IEEE Communications Magazine and IEEE Communications Letters. He has served as the chair, the TPC chair, and a TPC member for several premier IEEE conferences. In 2017, he has been appointed as Distinguished Visitor Speaker from the IEEE Computer Society and he has been elected treasurer of the IEEE ComSoc/VT Italy Chapter. In 2019, he has been also appointed as a member of the IEEE New Initiatives Committee from the IEEE Board of Directors and, in 2023, he has been appointed as ComSoc Distinguished Lecturer.